scientific reports

Check for updates

OPEN

Dopamine influences attentional rate modulation in Macaque posterior parietal cortex

Jochem van Kempen[1]✉, Christian Brandt[2,3], Claudia Distler[4], Mark A. Bellgrove[5] & Alexander Thiele[1]

Cognitive neuroscience has made great strides in understanding the neural substrates of attention, but our understanding of its neuropharmacology remains incomplete. Although dopamine has historically been studied in relation to frontal functioning, emerging evidence suggests important dopaminergic influences in parietal cortex. We recorded single- and multi-unit activity whilst iontophoretically administering dopaminergic agonists and antagonists while rhesus macaques performed a spatial attention task. Out of 88 units, 50 revealed activity modulation by drug administration. Dopamine inhibited firing rates according to an inverted-U shaped dose–response curve and increased gain variability. D1 receptor antagonists diminished firing rates according to a monotonic function and interacted with attention modulating gain variability. Finally, both drugs decreased the pupil light reflex. These data show that dopamine shapes neuronal responses and modulates aspects of attentional processing in parietal cortex.

Selective attention refers to prioritization of behaviorally relevant, over irrelevant, sensory inputs. Convergent evidence from human neuropsychological, brain imaging and non-human primate studies shows that fronto-parietal networks are crucial for selective attention[1–3]. Neuromodulation of attention-related activity in these networks occurs at least in part via glutamatergic[4,5] and cholinergic inputs[6–13]. Multiple lines of evidence, however, also suggest dopaminergic modulation[14–17]. Here we sought to understand how dopamine (DA) applied to macaque posterior parietal cortex (PPC) modulates attention-related activity.

The functional significance of DA is well established for a number of brain areas, particularly the frontal cortex (executive control) and basal ganglia (motor control). For these regions, substantial across-species similarities allowed the development of mechanistic models with clinical translational value for various disorders (e.g., Parkinson's disease, schizophrenia or attention deficit hyperactivity disorder (ADHD))[15,18]. Species differences with respect to dopaminergic innervation do however exist for posterior cortical areas, including the PPC. Although sparse in rodents, dopaminergic innervation of parietal areas in non-human primates is comparable in strength and laminar distribution to prefrontal regions[19]. Moreover, macaque PPC has high densities of DA transporter (DAT) immunoreactive axons[20]. These observations align with dense dopaminergic receptor expression in human PPC[21] and imaging studies of clinical disorders where medications targeting DA receptors or transporters modulate parietal activity[22]. Given these data and the clinical significance of PPC function, greater understanding of dopaminergic effects in this region is warranted.

Selective attention relies heavily on PPC integrity and multiple lines of evidence suggest that DA modulates attentional processes related to parietal function. First, DA agonists reduce spatial inattention in neurological[23] and psychiatric patients with disorders such as schizophrenia[24] and ADHD[25,26]. Second, psychopharmacological studies in healthy volunteers suggest that DA antagonists modulate parameters of spatial cueing paradigms (e.g. validity effect), often associated with parietal function[27]. Third, DNA variation in a polymorphism of the DA transporter gene (DAT1) is associated with individual differences in measures of spatial selective attention[28–30]. Fourth, non-human primate studies revealed dopaminergic contributions to working memory signals in dorsolateral prefrontal cortex (dlPFC)[31], and modulation of dopaminergic signaling in frontal eye fields (FEF) affects V4 neurons in a manner similar to attention and biases behavioral choices[16,17]. DA thus contributes to working memory, target selection and probably also spatial attention in dlPFC and FEF[16,31–33]. Both areas are critical

[1]Biosciences Institute, Newcastle University, Newcastle upon Tyne NE1 7RU, UK. [2]Research Unit for ORL – Head and Neck Surgery and Audiology, Odense University Hospital, Odense, Denmark. [3]University of Southern Denmark, Odense, Denmark. [4]Allgemeine Zoologie Und Neurobiologie, Ruhr-Universität Bochum, 44801 Bochum, Germany. [5]Turner Institute for Brain and Mental Health, School of Psychological Sciences, Monash University, Melbourne, VIC 3800, Australia. ✉email: vankempen.jochem@gmail.com

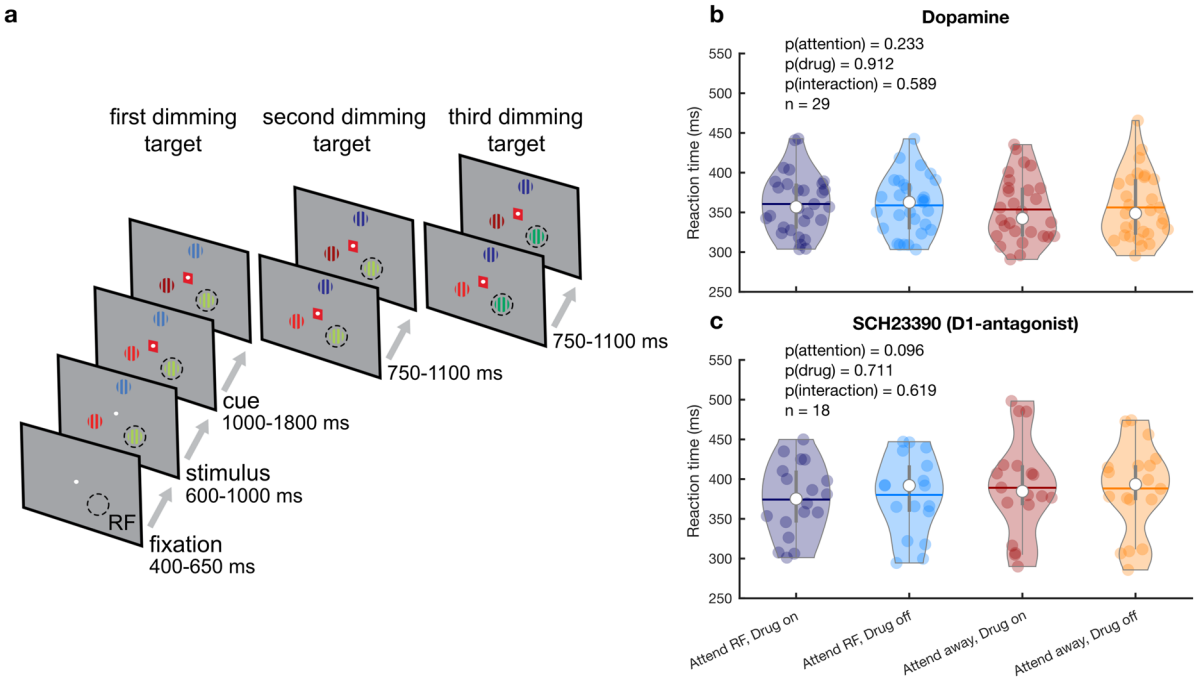

Figure 1. Paradigm and behavioral performance. (**a**) Behavioral paradigm. The monkey held a lever and fixated on a central fixation spot to initiate the trial. One of three colored gratings was presented inside the receptive field (RF) of the neurons under study. After a variable delay a cue matching one of the grating colors surrounded the fixation spot, indicating which grating was behaviorally relevant (target). In pseudorandom order the stimuli decreased in luminance (dimmed). Upon dimming of the target, the monkey had to release the lever to obtain a reward. (**b, c**) Average RT on attend RF and attend away trials for the non-specific agonist dopamine (**b**) and the D1R antagonist SCH23390 (**c**). Individual markers represent the average RT during a single recording session. Error bars denote the interquartile range. Horizontal bars denote the mean. Statistics: linear mixed-effects model analysis.

nodes of fronto-parietal attention networks. In summary, while dopaminergic influences on frontal circuits are comparatively well understood, their effect on attention-related activity in PPC is yet to be established.

Here we sought to address this knowledge gap by locally infusing DA or the selective D1 receptor (D1R) antagonist SCH23390 into the PPC of two macaque monkeys during a selective attention task. We show that single and multi-unit (SU, MU) activity is inhibited by iontophoresis of dopaminergic drugs into intraparietal sulcus (IPS) gray matter and that drug application increased trial-to-trial excitability fluctuations, termed gain variability[34]. The effects of the non-selective agonist DA followed an inverted U-shaped dose–response curve, whereas the dose–response curve of the D1-selective antagonist SCH23390 followed a monotonic function. Our data also tentatively suggest cell type specific effects of DA receptor manipulation on different aspects of attentional activity modulation, although these results are based on small sample sizes. Finally, both drugs reduced the pupillary light reflex.

Results

We recorded activity from 88 single and multi-units from intraparietal sulcus (IPS) in two awake, behaving Macaque monkeys performing a selective attention task (Fig. 1a). Of these units, 74 (84.1%) were modulated by attention, as measured during the 500 ms before the first dimming event (see Fig. 2). During recording, we used an electrode-pipette combination to iontophoretically administer dopaminergic drugs (using an ejection current range of 20–90 nA) in the vicinity of the recorded cells[35]. Across the two monkeys, we recorded from 59 units whilst administering the unselective agonist DA and from 29 units during which we administered the selective D1R antagonist SCH23390. Firing rates in 36 (61%) and 14 (48.3%) units were modulated by application of DA and SCH23390, respectively. Of these drug-modulated units, 31 (52.5%) and 14 (48.3%) were also modulated by attention. Thus, approximately half the total units were modulated both by attention and drug application. These proportions are comparable to cholinergic modulation of attention induced activity in macaque V1 and FEF[6,13], and glutamatergic modulation in FEF[5]. As expected given the focal nature of micro-iontophoretic drug application[36], and in line with comparable studies[37,38], there were no behavioral effects of drug application (i.e., reaction times) (Fig. 1b, c).

Dopaminergic drug application inhibits population activity. Figure 2a illustrates the population activity (from all units) aligned to stimulus onset, cue onset and the first-dimming event, for both the no-drug and the drug conditions. For a given drug condition, neural activity between attention conditions did not differ when aligned to stimulus onset but started to diverge approximately 200 ms after cue onset, indicating which of

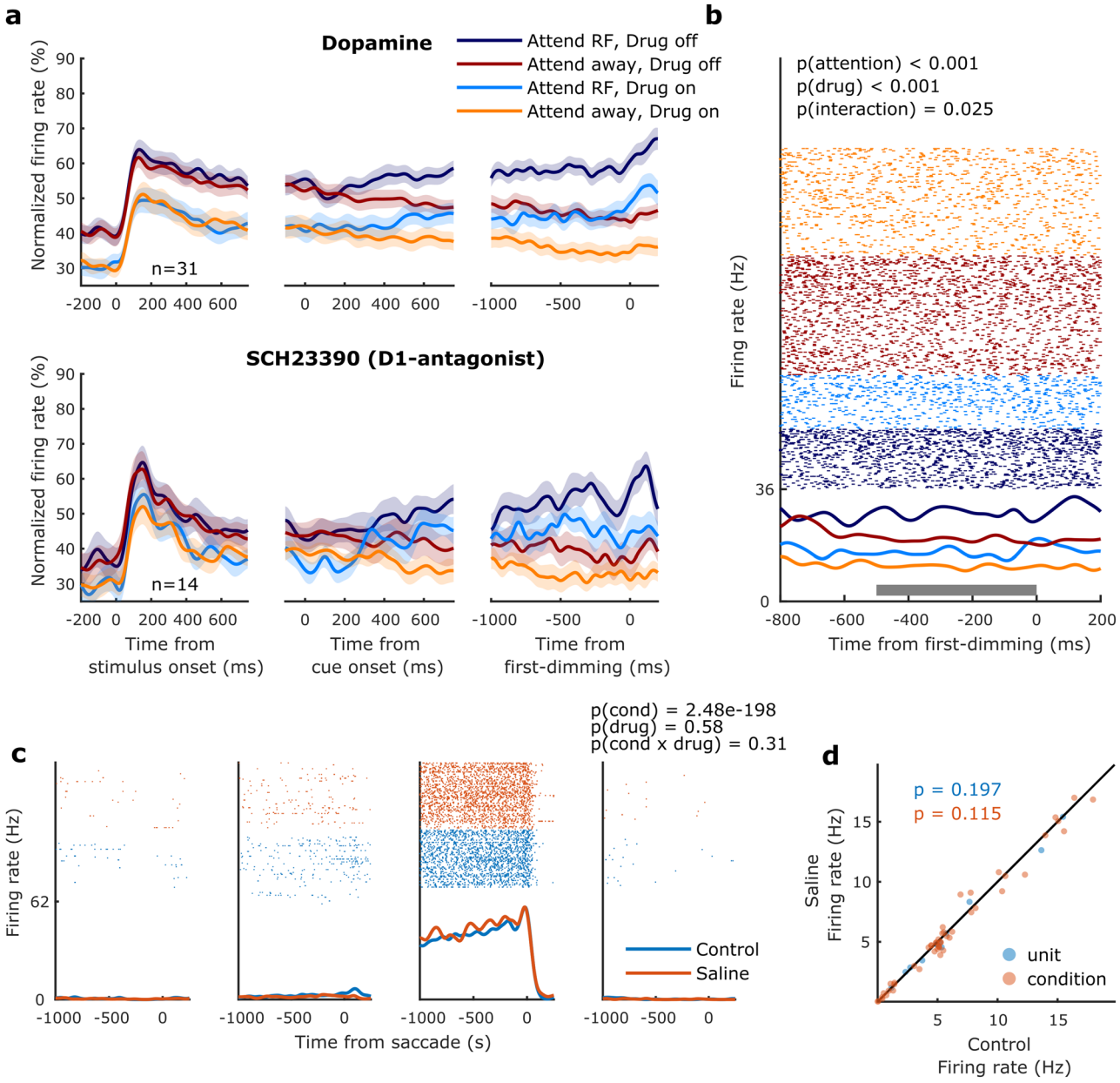

Figure 2. Population activity, example unit, and saline control. (**a**) Population histograms for all units recorded during dopaminergic drug application selective for attention and drug application. Population activity aligned to stimulus onset (left), cue onset (middle) and the first dimming event (right), for the non-specific agonist dopamine (top) and the D1R antagonist SCH23390 (bottom). Activity is normalized for each unit by its maximum activity. Error bars denote ± 1 SEM. (**b**) Activity from a cell recorded during dopamine application. This cell's activity, aligned to the first dimming event, was significantly modulated by attention, drug application and showed a significant interaction between these factors. The grey bar indicates the time window used for statistical analyses. Statistics: two-factor ANOVA. (**c**) Activity from a representative cell recorded during application of saline (with pH matched to the dopaminergic drugs) whilst the monkey performed a memory-guided saccade task. The four panels correspond to the four quadrants in which the visual stimulus was presented. This cell's activity, aligned to saccade onset, was significantly modulated by the spatial location of the stimulus/saccade but not by iontophoretic saline application. Statistics: two-factor ANOVA. (**d**) Average firing rates between control and saline conditions. Each marker indicates the average activity of one unit across the four conditions (blue markers) or the average activity of one unit for one of the four conditions (red markers). Statistics: two-sided Wilcoxon signed rank test.

the three gratings was behaviorally relevant on that trial, and diverged further leading up to the first dimming event. Across the population, DA strongly reduced firing rates throughout the duration of the trial, including

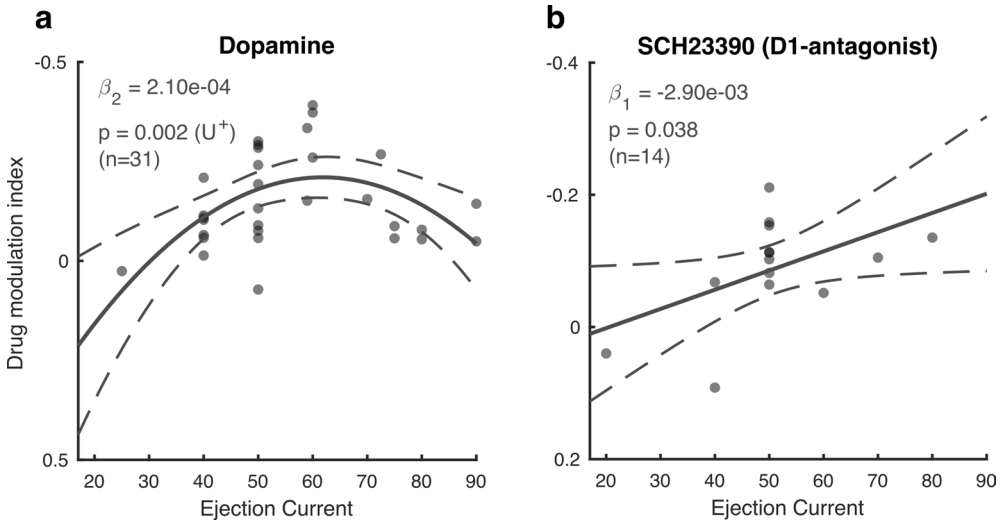

Figure 3. Dose–response curves. (**a, b**) Drug modulation index plotted against ejection current for the non-specific agonist dopamine (**a**) and the D1R antagonist SCH23390 (**b**). Note the reversed y-axis. Solid and dotted lines represent significant model fits (applied to all cells simultaneously) and their 95% confidence intervals, respectively. A monotonic relationship is shown if a first-order fit was better than a constant fit, and a non-monotonic relationship is shown if a second-order fit was better than a linear fit. U^+ indicates a significant U-shaped relationship. Only cells that revealed a main or interaction effect for the factors drug and attention were included in this analysis. Statistics: linear mixed-effects model analysis.

during baseline periods as well as stimulus and cue presentation. The effects of SCH23390 were of the same sign but weaker. Control recordings (saline with matched pH) to control for pH or current related effects did not reveal any effects on firing rates (Fig. 2c, d), and thus exclude the possibility that drug effects were the result of recording or application methods. Although drug induced changes to attentional modulation of neural activity appear relatively small at the population level, a subset of neurons revealed an interaction between attention and drug application ($n = 9$), as illustrated for an example neuron in Fig. 2b (further delineated below). Next, we examined the dose–response relationship between drug application and firing rates.

Dopaminergic drug dose–response curves. We applied dopaminergic drugs with a variety of iontophoretic ejection currents (20–90 nA). Since DA has previously been shown to modulate neural activity according to an inverted U-shaped dose–response curve[39], with maximal modulation at intermediate DA levels, we tested whether the ejection current was predictive of the firing rate modulation associated with drug application, estimated by a drug modulation index ($MI_{drug,}$ Materials & Methods). Specifically, we used sequential linear mixed-effect model analyses and likelihood ratio tests to test for linear and quadratic trends. U-shaped trends were verified using the two-lines approach (Materials & Methods). DA displayed a non-monotonic relationship with MI_{drug} ($\chi^2_{(1)} = 9.89$, $p = 0.002$) and revealed an inverted U-shaped curve ($p < 0.05$) in which intermediate ejection currents elicited the most negative MI_{drug}, i.e. the largest inhibition of activity (Fig. 3a). For SCH23390, on the other hand, we found a monotonic dose–response relationship ($\chi^2_{(1)} = 4.31$, $p = 0.038$), with more inhibition of firing rates with higher drug ejection currents (Fig. 3b). Neither of these dose–response relationships were dependent on unit sub-selection based on their attention or drug selectivity (Supplementary Figure S1).

Dopaminergic drug application modulates firing rates and rate variability. We tested whether DA application affected firing rates or rate variability, as quantified by the Fano Factor (FF) and gain variability. FF measures the variance of firing rate relative to the mean, and could capture drug induced changes if this relationship was linear. However, given the non-linear relationship (e.g. 40), it may not capture changes in excitability when mean rates change. Gain variability captures variability induced by changes in excitability that are independent of mean firing rates (additional detail see methods and 34, 40). These parameters were measured during the 500 ms preceding the first dimming, using linear mixed-effect models with categorical (effect coded) factors of drug (on/off) and attention (RF/away) (Fig. 4). Confidence intervals were computed across 5000 bootstrap replicates. To control for Type I errors and to aid interpretation of model fit statistics, we additionally report the Kenward-Roger approximation for performing F tests as well as the Bayes factor (Materials and methods). For firing rates, we found a main effect of attention ($\beta = 2.69 \pm 0.39$, 95% confidence interval = [1.94, 3.47], $\chi^2_{(1)} = 29.2$, $P = 5e^{-10}$, $P_{KR} = 8.19e^{-8}$, $BF = 6.65e^6$) reflecting the firing rate increase when attention is directed towards the RF, and a main effect of drug ($\beta = -2.36 \pm 0.39$, 95% confidence interval = [−3.13 −1.59], $\chi^2_{(1)} = 31.1$, $P = 2.44e^{-8}$, $P_{KR} = 3.74e^{-8}$, $BF = 2.06e^7$), indicating that DA application reduced firing rates (Fig. 4a). We did not find an interaction effect between attention and DA application. For FF (Fig. 4b), we did not find any main or interaction effects of attention or drug application. For gain variability, we found a small main effect of attention ($\beta = -0.09 \pm 0.04$, 95% confidence interval = [−0.17, −0.06], $\chi^2_{(1)} = 3.26$, $P = 0.039$, $P_{KR} = 0.07$, $BF = 0.6$)

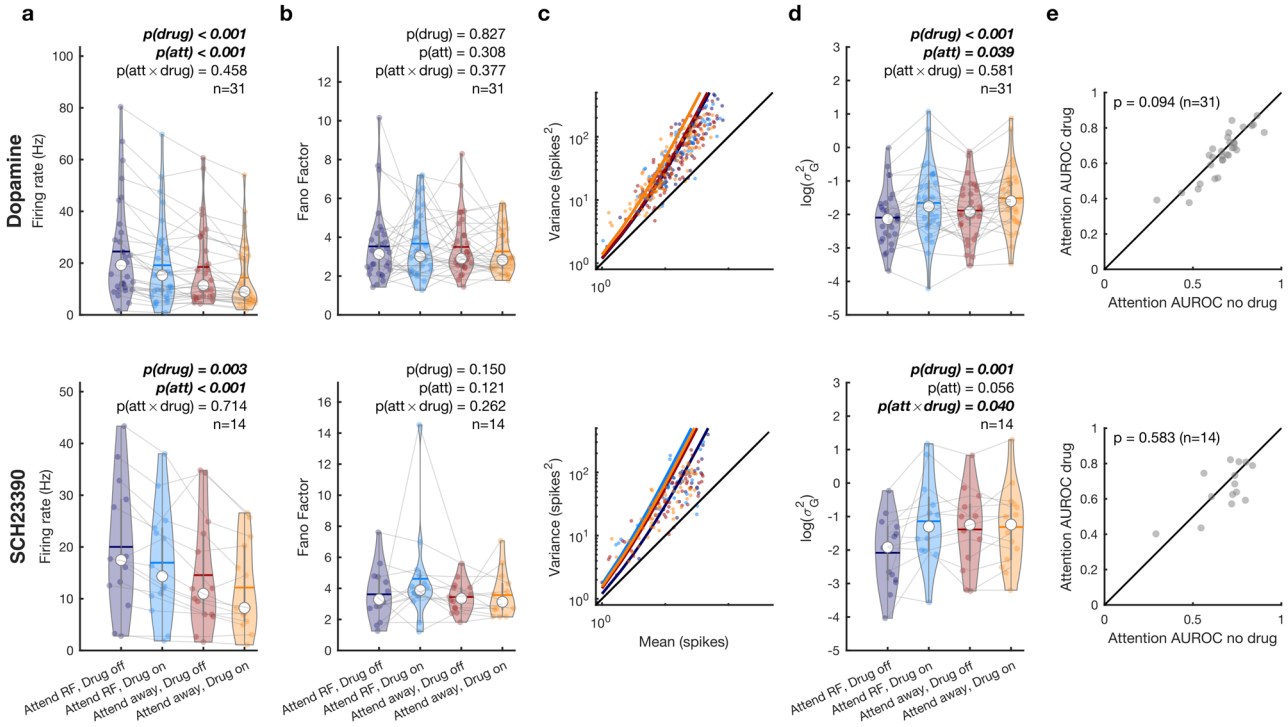

Figure 4. Dopaminergic modulation of firing rates and rate variability. (**a**) Average firing rates between attention and drug conditions for the non-specific agonist dopamine (top) and the D1R antagonist SCH22390 (bottom) (**b**) Fano factors between attention and drug conditions for the non-specific agonist dopamine (top) and the D1R antagonist SCH22390 (bottom). (**c**) Variance-to-mean relationship across attention and drug conditions for the non-specific agonist dopamine (top) and the D1R antagonist SCH22390 (bottom). Individual dots depict the variance and mean across trials for a single condition. Solid lines show the predicted mean-to-variance relationship given the average fitted dispersion parameter (σ_G^2). (**d**) Gain variability (σ_G^2) for each unit between attention and drug conditions for the non-specific agonist dopamine (top) and the D1R antagonist SCH22390 (bottom). (**e**) Area under the receiver operating characteristic (AUROC) curve between no drug and drug conditions for the non-specific agonist dopamine (top) and the D1R antagonist SCH23390 (bottom). Only units that revealed a main or interaction effect for the factors drug and attention were included in this analysis. Individual markers represent the average firing rate, Fano Factor or gain variability for a single unit (**a**, **b**, **d**). The white marker denotes the median and the error bars the interquartile range. Horizontal bars denote the mean. Statistics: linear mixed-effect models (**a, b, d**) and two-sided Wilcoxon signed rank test (**e**).

and a strong main effect of drug application ($\beta = 0.19 \pm 0.04$, 95% confidence interval = [0.11, 0.27], $\chi^2_{(1)} = 18.5$, $P = 1.7e^{-5}$, $P_{KR} = 2.33e^{-5}$, BF = 13,849.58) but no interaction. These results indicate the decrease in gain variability when attention was directed towards the RF and an increase in variability upon drug application (Fig. 4c, d).

We performed the same analyses for the application of SCH23390. For firing rates, we found a main effect of attention ($\beta = 2.56 \pm 0.44$, 95% confidence interval = [1.69, 3.43], $\chi^2_{(1)} = 20.9$, $P = 8.78e^{-7}$, $P_{KR} = 7.21e^{-6}$, $BF = 3.22e^4$) reflecting the firing rate increase when attention is directed towards the RF, and a main effect of drug ($\beta = -1.37 \pm 0.44$, 95% confidence interval = [−2.25, −0.49], $\chi^2_{(1)} = 8.47$, $P = 0.004$, $P_{KR} = 0.005$, BF = 13.3), indicating that SCH23390 application reduced firing rates (Fig. 4a). We did not find an interaction between attention and drug application. We did not find any effect of drug application or attention for FF (Fig. 4b), but for gain variability we found a trending main effect of attention ($\beta = -0.14 \pm 0.07$, 95% confidence interval = [−0.28, $2.2e^4$], $\chi^2_{(1)} = 3.52$, $P = 0.06$, $P_{KR} = 0.07$, BF = 1.08), a main effect of drug application ($\beta = 0.24 \pm 0.07$, 95% confidence interval = [0.10, 0.38], $\chi^2_{(1)} = 9.04$, $P = 0.002$, $P_{KR} = 0.004$, BF = 37.0) as well as an interaction between attention and drug application ($\beta = 0.15 \pm 0.07$, 95% confidence interval = [0.01, 0.30], $\chi^2_{(1)} = 4.22$, $P = 0.042$, $P_{KR} = 0.051$, BF = 0.98). Similar to the application of DA, these results indicate a decrease in gain variability when attention was directed towards the RF and an increase in variability upon drug applications (Fig. 4c, d). However, unlike after DA application, gain variability only increased upon application of SCH22390 when attention was directed towards the RF, but not when it was directed away, as indicated by follow up rank tests (two-sided Wilcoxon signed-rank test; attend RF: $P = 0.009$, Cohen's d = −0.82; attend away: $P = 0.244$, Cohen's d = −0.15).

Dopaminergic drug application and its effect on attention AUROC. To investigate whether DA affected attention-specific activity, we tested if attention AUROC values were modulated by drug application (Fig. 4e). Attention AUROC values indicate how well an ideal observer can distinguish between neural activity during attend RF or attend away trials. A value of 0.5 indicates that the distributions are indistinguishable, whereas values of 0 or 1 indicate perfectly distinguishable distributions. We found a trending reduction of

AUROC values upon dopamine application [two-sided Wilcoxon signed-rank test: Δ-AUROC −0.02 ± 0.01, $p = 0.094$, Cohen's d = −0.28]. SCH23390 application did not modulate AUROC values ($p = 0.58$).

To investigate whether drug dosage was also predictive of attentional rate modulation, we performed the sequential linear mixed-effect model analyses and likelihood ratio tests on the difference score (drug–no drug) of attention AUROC values to test for linear and quadratic trends. Neither DA ($\chi^2_{(1)} = 0.95$, $p = 0.330$), nor SCH23390 ($\chi^2_{(1)} = 0.33$, $p = 0.568$) dosage were predictive of attention AUROC, regardless of unit sub-selection (Supplementary Figure S2).

Cell type specific effects of dopamine receptor modulations. We additionally conducted the rate, variability and attentional AUROC analyses, grouping units by the width of their spike waveform, i.e. subdividing them into narrow and broad spiking cells (Methods, Supplementary Figure S3, S4 and S5). We report the outcome of this analysis in supplementary materials, as the resulting sample sizes were small, and hence statistical power was limited. Briefly, subdividing units into broad and narrow spiking classes, we found that DA affected attention-related AUROC values in broad-spiking, but not narrow-spiking units. SCH23390 application affected attention-related gain variability changes in broad-spiking units only. For details see supplementary materials.

Dopaminergic drug application decreases the pupillary light reflex. Interestingly, we found that the application of both DA and SCH23390 influenced pupil diameter. We conducted a sliding-window Wilcoxon signed rank test analysis for each 200 ms window, in 10 ms increments, comparing baseline-normalized pupil diameter on drug compared to no-drug trials (Fig. 5a). This analysis revealed a significant difference in pupil diameter that started after stimulus onset and lasted until after cue onset. Specifically, we found a small but significant modulation of the pupillary light reflex (Fig. 5). The magnitude of the constriction of the pupil was reduced during dopaminergic drug application compared to control trials upon stimulus onset [two-sided Wilcoxon signed-rank test; DA: Δ-pupil 0.10 ± 0.02, $p < 0.001$, Cohen's d = 1.09; SCH23390: Δ-pupil 0.10 ± 0.03, $p = 0.004$, Cohen's d = 0.79], but neither drug influenced pupil diameter during any other time window (no other effects survived FDR correction) (Fig. 5b–e). Another sliding window analysis using a two factor (drug by attention) repeated measures ANOVA revealed no effect of attention (main or interaction) on pupil diameter (data not shown). Thus, locally applied dopaminergic drugs in parietal cortex modulated the pupillary light reflex upon stimulus onset.

Discussion

We tested the effects of dopaminergic drugs on PPC activity during spatial selective attention. The non-specific agonist DA inhibited activity according to an inverted U-shaped dose–response curve, whereas the D1R antagonist SCH23390 decreased firing rates following a monotonic dose–response curve. Attention and DA application affected gain variability, and SCH23390 application resulted in increased gain variability during attend RF but not attend away conditions. We report preliminary evidence that DA reduces attention-related firing rate modulations in broad-spiking units. Finally, we found that local drug application in parietal cortex decreased the pupillary light reflex. This is the first study (to the best of our knowledge) revealing the role of dopaminergic modulation on task-related activity in the parietal cortex of the rhesus macaque.

Dopaminergic modulation in parietal cortex. DA has a well-established role in modulating prefrontal signaling, supporting cognitive functions such as working memory and attention[15,31–33,39,41,42]. D1R and D2R are expressed broadly throughout the cortex and fulfil complementary roles in prefrontal cognitive control[42]. Although D2Rs have been implicated in rule coding[43], modulation of working memory is mostly associated with D1R stimulation or blockade[31,44–46]. Moreover, while manipulation of either receptor subtype in FEF can modulate behavioral choices[17], only D1R blockade in FEF elicits activity resembling attentional effects in extrastriate visual areas[16]. Interestingly, D1R expression is higher in FEF pyramidal cells compared to interneurons[47,48]. In our sample, the effects of dopaminergic drugs were greater for broad-, rather than narrow-spiking units (supplementary materials). Although it is unknown whether DA receptor expression differs across cell types in PPC, if expression is similar to the FEF, modulation of parietal attentional signals might rely on higher expression of D1R compared to D2R in broad-spiking putative pyramidal cells.

It is remarkable that the majority of the recorded neurons were inhibited by DA and SCH23390 application, as previous studies (in prefrontal cortex) found mixed responses to unselective DA[37] or D1R stimulation[31,39]. As control recordings using saline did not result in any systematic effects (Fig. 2c, d), these effects were not due to our recording/iontophoresis methods.

The effects found may alternatively be explained by drug dosages. Although Jacob et al.[37] found that the proportion of inhibited and excited cells did not differ across a variety of ejection currents (25–100 nA), activity increases have been found for low, and decreases for high D1R agonist and antagonist dosages[31,39]. Indeed, while our sample size using lower dosages was small, lower ejection currents predicted positive and less negative modulation. At the dosages used in this study, DA could have mostly inhibitory effects. Vijayraghavan et al.[39] found that low doses (10–20 nA) of D1R agonists reduced overall firing rates, but increased spatial specificity of prefrontal neurons, whereas high dosages (20–100 nA) further reduced activity and abolished spatially selective information. Given that our study was unrelated to spatial specificity (i.e. saccade field tuning), we were unable to assess this particular feature, but dopaminergic influences may still enhance spatial tuning of PPC despite an overall reduction in activity.

Another factor that could explain the low number of DA-excited units is the short block duration used in our task. Cells excited by DA respond more slowly to drug application than inhibited cells, with an average modulation up-ramp time constant of 221.9 s[37]. In our task, with a median trial duration of approximately 8 s, a block

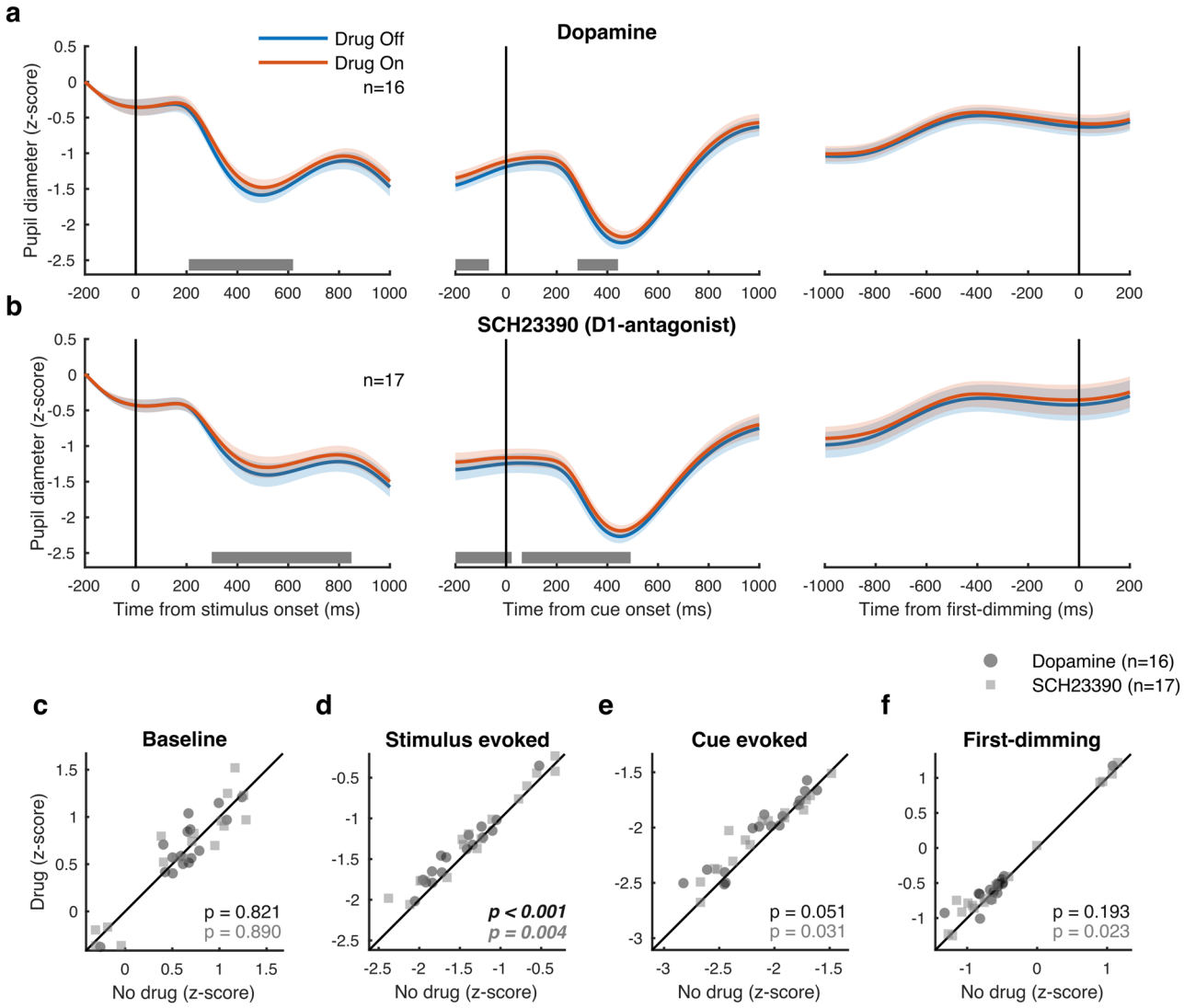

Figure 5. Modulation of pupil diameter by dopamine in parietal cortex. (**a**) Pupil diameter during sessions where dopamine was administered aligned to stimulus onset (left), cue onset (middle) and the first dimming event (right). The grey bar indicates the times where drug application brought about a significant difference in pupil diameter. (**b**) As (**a**) but for sessions where D1R antagonist SCH23390 was applied. (**c**–**f**) Average pupil diameter during pre-stimulus baseline period (**c**), after stimulus onset (**d**), after cue onset (**e**), and before the first dimming event (**f**). Shaded regions denote ± 1 SEM. Statistics: Wilcoxon signed rank test (FDR corrected). Statistics deemed significant after multiple comparison correction are displayed in italic and boldface fonts.

(36 trials) lasted approximately 288 s. DA-excited neurons could have only started to show modulation towards the end of the block, resulting in a population of largely inhibited units.

In sum, dopaminergic effects on (task-related) activity are complex[49] and depend on various factors not controlled for in this study, such as endogenous levels of DA. Within prefrontal cortex, coding can be enhanced by D1R agonists, and diminished by antagonists[39,43], or vice-versa[16,31]. Indeed, dopaminergic effects show regional variability across different brain areas, even within PFC[18]. Thus, the mechanisms discussed above might not apply to PPC. Finally, as SCH23390 also has high affinity agonistic properties for 5-HT_{2c} (serotonin) receptors[50], some of our effects might be unrelated to dopaminergic functioning. Although the effects on attention were modest and our sample size was relatively small, these results encourage future studies with larger sample sizes and a more detailed distinction between cell types to explore cell-type and receptor-subtype specific (dose-dependent) effects of DA in parietal cortex during task performance.

Dopaminergic dose–response curve. DA receptor stimulation follows an inverted-U shaped dose–response curve whereby too little or too much stimulation leads to suboptimal behavioral performance[51,52] or neural coding[39]. Whereas optimal levels of DA receptor stimulation can stabilize and tune neural activity, suboptimal levels decrease neural coding and behavioral performance.

Here we found an inverted-U shaped dose–response curve for DA, and a monotonic function for SCH23390. Rather than predicting neural coding for attention, however, ejection currents were merely predictive of drug modulation indices, without any relationship to attention AUROC values (but see supplementary materials). However, these results should be interpreted with caution. First, our sample size, especially for SCH23390, might have been too small to reliably determine the shape of the dose–response curve. Second, since lower and higher ejection currents were not used as often as intermediate currents, it is possible we did not have sufficient data to constrain the function fit at the extremes. Finally, we applied different ejection currents across rather than within cells. Based on these data, it is therefore not possible to conclusively state that individual cells in parietal cortex respond according to a U-shaped dose response curve. It is furthermore important to note that the dopaminergic effects might partly be driven by receptor subtypes (e.g. D2R) not usually associated with modulation of delay period activity. Despite these notes of caution, we believe this study provides evidence for a role of DA in parietal cortex during cognitive tasks and presents opportunities for future research to elucidate the exact underlying mechanisms.

Dopaminergic modulation of the pupil light reflex. The pupil light reflex (PLR) transiently constricts the pupil after exposure to increases in illumination or presentation of bright stimuli[53,54]. Recent studies have shown that covert attention can modulate this behavioral reflex[55–57]. Subthreshold FEF microstimulation respectively enhances or reduces the PLR when a light stimulus is presented inside or outside the saccade field[58]. The PLR thus depends both on luminance changes and the location of spatial attention. We found that dopaminergic drug application in parietal cortex reduced the PLR. Two (non-exclusive) mechanisms have been proposed by which FEF can modulate the PLR[59]; by direct or indirect projections to the olivary pretectal nucleus, or via indirect projections to constrictor neurons in the Edinger-Westphal nucleus. For the latter, these projections are hypothesized to pass through extrastriate visual cortex and/or the superior colliculus (SC). Subthreshold microstimulation of the intermediate (SCi), but not superficial (SCs), layers of the SC elicits a short latency pupillary dilation[60,61]. Whereas the SCs receive input from early visual areas, including the retina, the SCi receives input from higher-order association cortices. Along with preparing and executing eye movements, the SCi is involved in directing covert attention[62–65], and provides an essential contribution to the selection of stimuli amongst competing distractors[66–68]. Moreover, the SC receives dense projections from parietal cortex[69,70], and has been hypothesized to play an important role in pupil diameter modulation[71]. It is currently unclear whether dopaminergic modulation of frontal (or parietal) cortex modulates SC activity, but this pathway seems a strong candidate for the modulation of the PLR[71] that we encountered in this study through DA application. Here, dopaminergic drug application reduced parietal activity and brought about a gain modulation (reduction) of a brainstem-mediated reflex to fixed visual input. Although covert attention was not directed at any specific stimulus at the time of stimulus onset, the modulation of the PLR observed here is consistent with previously reported effects of covert attention and FEF microstimulation on the PLR. Speculatively, this modulation could affect the bottom-up attentional capture by the stimulus, but further studies are required to test this hypothesis.

Conclusion

DA is an important modulator of high-level cognitive functions, both in the healthy and ageing brain as well as for various clinical disorders[15,18,72]. Although dopaminergic effects within PFC have been elucidated in some detail, the effects of DA in other brain areas such as parietal cortex, despite its well-established role in cognition and cognitive dysfunction, has largely been overlooked. This study is the first to show dopaminergic modulation of parietal activity in general, and activity specific to spatial attention in the non-human primate. Our work encourages future studies of dopaminergic involvement in parietal cortex, thereby gaining a broader understanding of neuromodulation in different networks for cognition.

Materials and methods

Procedures. All animal procedures were approved by the Newcastle University Animal Welfare Ethical Review Board and performed in accordance with the European Communities Council Directive RL 2010/63/EC, the National Institute of Health's Guidelines for the Care and Use of Animals for Experimental Procedures, and the UK Animals Scientific Procedures Act. Animals were motivated to engage in the task through fluid control at levels that do not affect animal physiology and have minimal impact on psychological wellbeing[73].

Surgical preparation. The monkeys were implanted with a head post and recording chambers over the lateral intraparietal sulcus under sterile conditions and under general anesthesia. Surgery and postoperative care conditions have been described in detail previously[35].

Behavioral paradigms. Stimulus presentation and behavioral control was regulated by Remote Cortex 5.95 (Laboratory of Neuropsychology, National Institute for Mental Health, Bethesda, MD). Stimuli were presented on a cathode ray tube (CRT) monitor at 120 Hz, 1280 × 1024 pixels, at a distance of 54 cm.

The location of the saccade field (SF) was mapped using a visually- or memory-guided saccade task. Here, monkeys fixated centrally for 400 ms after which a saccade target was presented in one of nine possible locations (8–10° from fixation, distributed equidistantly). After a random delay (800–1400 ms, uniformly distributed) the fixation point was extinguished, which indicated to the monkey to perform a saccade towards the target. In the memory-guided version of the task (used only for saline-control recordings), the visual target was briefly presented in one of four locations. After extinguishing the target, its location needed to be remembered until a saccade was made towards the remembered location (after extinguishing of the fixation point). Online analysis of visual, sustained and saccade related activity determined an approximate SF location which guided our

	Red	Green	Blue
Monkey 1 Early recordings ($n = 29$)	a. [255 0 0]–14.5	a. [0 128 0]–9.1	a. [60 60 255]–11.5
	b. [100 0 0]–1.4	b. [0 70 0]–1.9	b. [10 10 140]–2.2
Monkey 2 Early recordings ($n = 5$)	a. [220 0 0]–12.8	a. [0 135 0]–12.9	a. [60 60 255]–12.2
	b. [180 0 0]–7.7	b. [0 110 0]–7.3	b. [35 35 220]–7.4
Monkey 1/2 ($n = 12/8$) Late recordings	a. [220 0 0]–12.8	a. [0 135 0]–12.9	a. [60 60 255]–12.2
	b. [140 0 0]–4.2	b. [0 90 0]–4.6	b. [30 30 180]–4.6

Table 1. Color values used for the 3 colored gratings across recording sessions and subjects, indicated as [RGB]—luminance (cd/m^2). a = Undimmed values, b = dimmed values.

subsequent receptive field (RF) mapping. The location and size of RFs were measured as described previously[74], using a reverse correlation method. Briefly, during fixation, a series of black squares (1–3° size, 100% contrast) were presented for 100 ms at pseudorandom locations on a 9 × 12 grid (5–25 repetitions for each location) on a bright background. RF eccentricity ranged from 2.5° to 17° and were largely confined to the contralateral visual field.

The main task and stimuli have been described previously[40,75,76]. In brief, the monkey initiated a trial by holding a lever and fixating a white fixation spot (0.1°) displayed on a grey background (1.41 cd/m^2). After 425/674 ms [monkey 1/monkey 2] three colored square wave gratings (2°–6°, dependent on RF size and distance from fixation) appeared equidistant from the fixation spot, one of which was centered on the RF of the recorded neuron. Red, green and blue gratings (see Table 1 for color values) were presented with an orientation at a random angle to the vertical meridian (the same orientation for the three gratings in any given session). The locations of the colors, as well as the orientation, were pseudorandomly assigned between recording sessions and held constant for a given recording session. Gratings moved perpendicular to the orientation, whereby the direction of motion was pseudorandomly assigned for every trial. After a random delay (570–830/620–940 ms [monkey 1/monkey 2], uniformly distributed in 1 ms steps) a central cue appeared that matched the color of the grating that would be relevant on the current trial. After 980–1780/1160–1780 ms [monkey 1/monkey 2] (uniformly distributed in 1 ms steps), one pseudorandomly selected grating changed luminance (dimmed). If the cued grating dimmed, the monkey had to release the lever to obtain a reward. If a non-cued grating dimmed, the monkey had to ignore this and wait for the cued grating to dim. This could happen when the second or third grating changed luminance (each after 750–1130/800–1130 ms [monkey 1/monkey 2], uniformly distributed in 1 ms steps). Drugs were administered in blocks of 36 trials. The first block was always a control block. Thereafter, drug blocks and recovery blocks were alternated until the animal stopped working (number of block reversals, median ± interquartile range = 12 ± 6).

Identification of recording sites. The location of the IPS was initially guided by means of postoperative structural magnetic resonance imaging (MRI), displaying the recording chamber. During each recording, neuronal response properties were determined using SF and RF mapping tasks. During the SF mapping task, we targeted cells that showed spatially selective persistent activity and preparatory activity before the execution of a saccadic eye movement.

Electrode-pipette manufacturing. We recorded from the lateral (and in a few occasions medial) bank of the IPS using custom-made electrode-pipettes that allowed for simultaneous iontophoretic drug application and extracellular recording of spiking activity[35]. The location of the recording sites in one of the monkeys was verified in histological sections stained for cyto- and myeloarchitecture[77].

The manufacture of the electrodes was similar to the procedures described by Thiele et al.[35], with minor changes to the design in order to reach areas deeper into the IPS, such as the ventral part of the lateral intraparietal area (LIPv). We sharpened tungsten wires (125 µm diameter, 75 mm length, Advent Research Materials Ltd., UK) by electrolytic etching of the tip (10–12 mm) in a solution of $NaNO_2$ (172.5 g), KOH (85 g) and distilled water (375 ml). We used borosilicate glass capillaries with three barrels (custom ordered, Hilgenberg GmBH, www.hilgenberg-gmbh.de), with the same dimensions as those described previously[35]. The sharpened tungsten wire was placed in the central capillary and secured in place by bending the non-sharpened end (approximately 10 mm) of the wire over the end of the barrel. After marking the location of the tip of the tungsten wire, shrink tubing was placed around the top and bottom of the glass. The glass was pulled around the tungsten wire using a PE-21 Narishige microelectrode puller with a heating coil made from Kanthal wire (1 mm diameter, 13 loops, inner loop diameter 3 mm) and the main (sub) magnet set to 30 (0) and the heater at 100. The electrode-pipette was placed such that the tip of the tungsten wire protruded 11 mm from the bottom of the heating coil. After pulling, we filled the central barrel (with the tungsten electrode inside) with superglue using a syringe and fine flexible injection cannula (MicroFil 28 AWG, MF28G67-5, World Precision Instruments, Ltd.). We found that if we did not fill (most of) the central barrel with superglue after pulling, the recorded signal was often very noisy, possibly due to small movements of the animal (such as drinking), which caused the free tungsten wire to resonate inside the glass. Using a micro grinder (Narishige EG-400), we removed excess glass, sharpened the tip of the electrode and opened the flanking barrels of the pipette. This pulling procedure resulted in a pulled

electrode part of approximately 2.5 cm length, with gradually increasing diameter, from ~ 10 to ~ 200 µm, over the first 12 mm of the electrode-pipette.

Electrode-pipette filling and iontophoresis. Electrode-pipettes were back-filled with the same drug in both pipettes using a syringe, filter units (Millex® GV, 22 µm pore diameter, Millipore Corporation) and fine flexible injection cannula (MicroFil 34 AWG, MF34G-5, World Precision Instruments, Ltd.). The pipettes were connected to the iontophoresis unit (Neurophore-BH- 2, Medical systems USA) with tungsten wires (125 µm diameter) inserted into the flanking barrels. Because of the exploratory nature of these recordings (it is unknown whether DA influences parietal neurons during spatial attention tasks and what modulation can be expected with different amounts of drug applied), we used a variety of iontophoretic ejection currents (20–90 nA). The choice of current was not based on the characteristics of individual cells (e.g. their responsiveness to the drug). A fixed ejection current of 50 nA was used for the saline-control recordings. The details regarding concentration and pH of the drugs were: DA (0.1 M in water for injections, pH 4–5), SCH23390 (0.005–0.1 M in water for injections, pH 4–5) and saline with citrate/hydrochloric acid buffer solution (pH 4). We excluded the first two trials after a block change to allow the drugs to wash in/out and avoid sudden rate changes.

Data acquisition. Stimulus presentation, behavioral control and drug administration was regulated by Remote Cortex 5.95 (Laboratory of Neuropsychology, National Institute for Mental Health, Bethesda, MD). Raw data were collected using Remote Cortex 5.95 (1-kHz sampling rate) and by Cheetah data acquisition (32.7-kHz sampling rate, 24-bit sampling resolution) interlinked with Remote Cortex 5.95. Data were replayed offline, sampled with 16-bit resolution and band-pass filtered (0.6–9 kHz). Spikes were sorted manually using SpikeSort3D (Neuralynx). Eye position and pupil diameter were recorded using a ViewPoint eyetracker (Arrington research) at 220 Hz. Pupil diameter was recorded in 33 out of 47 recording sessions.

Pupillometry. Pupil diameter was low pass filtered (10 Hz) using a second order Butterworth filter. Baseline activity, estimated as the average activity before stimulus onset (−300 to −50 ms), was subtracted from the pupil diameter time course on a trial-by-trial basis. Next, we z-score normalized the pupil diameter data for each session. Pupil diameter was averaged in 250 ms windows around 500 ms following stimulus onset, 500 ms following cue onset and between 300 and 50 ms before the first-dimming event.

Analysis of cell type. We distinguished between different cell types based on the duration of the extracellular spike waveform as described in Thiele et al.[40]. Specifically, we classified cells based on the peak-to-trough ratio, i.e. the duration between the peak and the trough of the interpolated (cubic spline) spike waveform. To test whether the distribution of peak-to-trough distance of the spike waveforms was unimodal (null hypothesis) or bimodal, indicating that our distribution contained different cell types, a modified Hartigan's dip test was used[40,78]. We used a cut-off of 250 µs to classify cells as narrow or broad-spiking, as this was where our distribution revealed the main 'dip' (Supplementary Figure S3a-b).

Fano factor. The variability of neural responses was quantified using Fano factors (*FF*), computed as the ratio between the variance (σ^2) and the mean (μ) spike counts within the time window of interest, defined as:

$$FF = \frac{\sigma^2}{\mu}$$

Drug modulation. The strength of the effect of drug application on neural activity (firing rates) was determined via a drug modulation index (*drugMI*), defined as:

$$drugMI = \frac{drug_{on} - drug_{off}}{drug_{on} + drug_{off}}$$

with $drug_{on}$ as the neural activity when drug was applied, and $drug_{off}$ the activity when the drug was not applied. This index ranges from -1 to 1, with zero indicating no modulation due to drug application and with positive values indicating higher activity when the drug was applied and conversely, negative values indicating lower activity.

Quantification of attentional rate modulation. To quantify the difference between neural responses when attention was directed towards the RF versus away from the RF, we computed the area under the receiver operating characteristic (AUROC) curve. Stemming from signal detection theory[79], this measure represents the difference between two distributions as a single scalar value, taking into account both the average difference in magnitude as well as the variability of each distribution. This value indicates how well an ideal observer would be able to distinguish between two distributions, for example the neural response when attention is directed towards versus away from its RF. It is computed by iteratively increasing the threshold and computing the proportion (from the first sample to the threshold) of hits and false alarms (FA), i.e. the correct and false classification as samples belonging to one of the activity distributions. The ROC curve is generated by plotting the proportions of hits against the proportion of FAs, and AUROC is taken as the area under the ROC curve. An AUROC of 0.5 indicates that the two distributions were indistinguishable, whereas an AUROC of 0 or 1 indicates that the two distributions were perfectly separable. As the difference from 0.5 indicates the separability of the

distributions, we corrected AUROC values (1-AUROC) for control and drug conditions when they were below 0.5 when no drugs (control) were applied, i.e. for those units that displayed higher activity when attention was directed towards the distractors compared to when attention was directed towards the RF.

Gain variability. Gain variability here is defined as variability that arises from (non-stimulus related) fluctuations in neuronal excitability. These fluctuations are a consequence of internal factors, such as changes in arousal, attention, and associated changes to excitatory/inhibitory and neuromodulatory drive. Thus the likelihood of a neuron firing is affected by external drive and by stimulus-independent modulatory influences on excitability ('gain')[34]. This 'gain' can change over time, hence the term 'gain variability'. Specifically, neural activity displays super-Poisson variability (larger variance than the mean), resulting from trial-to-trial changes in excitability, that can be modeled by fitting a negative binomial distribution to the spike rate histogram. This distribution is characterized by a dispersion parameter that captures this additional variability and has been proposed to reflect stimulus-independent modulatory influences on excitability[34]. For each unit, we fit the distribution of firing rates recorded during the 500 ms before the first dimming with a negative binomial distribution and obtained a gain variance (dispersion) term that captures trial-to-trial changes in excitability, separately for each drug and attention condition (but across stimulus direction conditions).

Experimental design and statistical analysis. All methods are reported in accordance with ARRIVE guidelines (https://arriveguidelines.org). We recorded single (SU, $n = 40$) and multi-unit (MU, $n = 48$) activity (total 88 units; 64 from monkey 1, 24 from monkey 2) from two male rhesus macaque monkeys (*Macaca mulatta,* age 9–11 years, weight 8–12.9 kg). We recorded an additional 12 units during saline-control recordings from one female macaque monkey (11 years, 9.1 kg). As the same experimenter performed preparations of the drugs, filling of the electrode-pipette, recording and analysis of the data, the investigators were not blinded to the drug type or ejection current. However, any parameters that could influence the behavior of the animal were minimized due to the blocked design of our experiment. The protocol for this study was not preregistered but closely followed previous approaches and methods used in our group.

We assessed the effect of drug application on the following parameters: firing rate, Fano Factor, gain variability, reaction time and pupil diameter. Activity for each unit was normalized by its maximum activity across any analyzed time window and condition. To determine whether DA significantly affected neural activity across the population of units, we used linear mixed-effect models using the R packages *lme4*[80] and *lmerTest*[81]. The modulation of neural activity (firing rates, Fano Factors or gain variability) was modeled as a linear combination of categorical (effect coded) factors drug (on/off), attention (RF/away), unit type (narrow/broad) and all possible interactions as fixed effects with random intercepts for each unit. We sequentially entered predictors into a hierarchical model and tested the model fit after the addition of each predictor using likelihood ratio tests. For small sample sizes, the χ^2 approximation employed in likelihood ratio tests can lead to misleading conclusions. We therefore additionally report the Kenward-Roger approximation for performing F tests to control for Type I errors[82–84] using the R package *pbkrtest*[82]. To aid interpretation of model fit statistics, we also report Bayes Factors, computed from the sample size, number of predictors and R^2 values[85,86] using the R package *BayesFactor*[87]. Finally, to confirm whether each of the measures had a significant effect on neural activity, we performed "robust regression" based on 5000 bootstrap replicates to calculate the 95% CI around slope estimates for the full model. The reported coefficients are the estimates from the full model and the robust regression. Reported significance values are the results from likelihood ratio tests. We followed these analyses up with linear mixed-effect model tests within each unit type and two-sided paired-sample Wilcoxon signed rank tests.

For comparisons within one recording, e.g. spike rates across trials for different conditions, we used analysis of variance (ANOVA) with three factors: attention (towards/away from the RF), drug (on/off) and stimulus direction. To test whether drug application affected behavioral performance, we used sequential linear mixed effects models with attention and drug as fixed effects and with the recording number as a random effect, to account for the repeated measurements in the data.

To test for significant linear or quadratic trends in the drug dose–response curve, we used sequential linear mixed effects models and likelihood ratio tests. For each drug, we tested whether a first order (linear) polynomial fit was better than a constant (intercept-only) fit and subsequently whether a second order (non-monotonic) polynomial fit was better than a linear fit. The modulation due to drug application of the neural response y was modeled as a linear combination of polynomial basis functions of the iontophoretic ejection current X:

$$y \sim \beta_0 + \beta_1 X + \beta_2 X^2,$$

with β as the polynomial coefficients. When a significant quadratic relationship was found, we used the two-lines approach to determine whether this relationship was significantly U-shaped[88].

Error bars in all violin plots indicate the interquartile range and the standard error of the mean (SEM) otherwise. We used false discovery rate (FDR) to correct for multiple comparisons.

We selected which cells to include in each of the analyses based on the output of the 3-factor ANOVA described above. For example, if we wanted to investigate whether drug application affected attentional modulation of firing rates, we only included cells that revealed a main or interaction effect for both attention and drug application.

Data and code availability

Data analyses were performed using custom written scripts in Matlab (the Mathworks) and RStudio (RStudio Team (2016). RStudio: Integrated Development for R. RStudio, Inc., Bos- ton, MA URL http://www.rstudio.com). Violin plots were created using publicly available Matlab code[89]. Analysis scripts necessary to reproduce these results are available at https://github.com/jochemvankempen/attention-parietal-dopamine and https://github.com/jochemvankempen/gain-variability, proccessed data are available at https://doi.org/10.12751/g-node.7ni115[90].

Received: 29 October 2021; Accepted: 11 April 2022
Published online: 28 April 2022

References

1. Corbetta, M. & Shulman, G. L. Spatial neglect and attention networks. *Annu. Rev. Neurosci.* **34**, 569–599 (2011).
2. Desimone, R. & Duncan, J. Neural mechanisms of selective visual attention. *Annu. Rev. Neurosci.* **18**, 193–222 (1995).
3. Posner, M. The attention system of the human brain. *Annu. Rev. Neurosci.* **13**, 25–42 (1990).
4. Herrero, J. L., Gieselmann, M. A., Sanayei, M. & Thiele, A. Attention-induced variance and noise correlation reduction in macaque v1 is mediated by NMDA receptors. *Neuron* **78**, 729–739 (2013).
5. Dasilva, M., Brandt, C., Alwin Gieselmann, M., Distler, C. & Thiele, A. Contribution of ionotropic glutamatergic receptors to excitability and attentional signals in macaque frontal eye field. *Cereb. Cortex* https://doi.org/10.1093/cercor/bhab007 (2021).
6. Herrero, J. L. *et al.* Acetylcholine contributes through muscarinic receptors to attentional modulation in V1. *Nature* **454**, 1110–1114 (2008).
7. Furey, M. L., Pietrini, P., Haxby, J. V. & Drevets, W. C. Selective effects of cholinergic modulation on task performance during selective attention. *Neuropsychopharmacology* https://doi.org/10.1038/sj.npp.1301461 (2008).
8. Parikh, V., Kozak, R., Martinez, V. & Sarter, M. Prefrontal acetylcholine release controls cue detection on multiple timescales. *Neuron* **56**, 141–154 (2007).
9. Nelson, C. L., Sarter, M. & Bruno, J. P. Prefrontal cortical modulation of acetylcholine release in posterior parietal cortex. *Neuroscience* **132**, 347–359 (2005).
10. Sarter, M., Hasselmo, M. E., Bruno, J. P. & Givens, B. Unraveling the attentional functions of cortical cholinergic inputs: interactions between signal-driven and cognitive modulation of signal detection. *Brain Res. Rev.* **48**, 98–111 (2005).
11. Levin, E. D. & Simon, B. B. Nicotinic acetylcholine involvement in cognitive function in animals. *Psychopharmacol. (Berl)* **138**, 217–230 (1998).
12. Warburton, D. M. & Rusted, J. M. Cholinergic control of cognitive resources. *Neuropsychobiology* **28**, 43–46 (1993).
13. Dasilva, M. *et al.* Cell class-specific modulation of attentional signals by acetylcholine in macaque frontal eye field. *Proc. Natl. Acad. Sci.* https://doi.org/10.1073/pnas.1905413116 (2019).
14. Bellgrove, M. A. & Mattingley, J. B. Molecular genetics of attention. *Ann. N. Y. Acad. Sci.* **1129**, 200–212 (2008).
15. Thiele, A. & Bellgrove, M. A. Neuromodulation of attention. *Neuron* **97**, 769–785 (2018).
16. Noudoost, B. & Moore, T. Control of visual cortical signals by prefrontal dopamine. *Nature* **474**, 372–375 (2011).
17. Soltani, A., Noudoost, B. & Moore, T. Dissociable dopaminergic control of saccadic target selection and its implications for reward modulation. *Proc. Natl. Acad. Sci. USA* **110**, 3579–3584 (2013).
18. Arnsten, A. F. T., Wang, M. J. & Paspalas, C. D. Neuromodulation of thought: flexibilities and vulnerabilities in prefrontal cortical network synapses. *Neuron* **76**, 223–239 (2012).
19. Berger, B., Gaspar, P. & Verney, C. Dopaminergic innervation of the cerebral cortex: unexpected differences between rodents and primates. *Trends Neurosci.* **14**, 21–27 (1991).
20. Lewis, D. A. *et al.* Dopamine transporter immunoreactivity in monkey cerebral cortex: regional, laminar, and ultrastructural localization. *J. Comp. Neurol.* **432**, 119–136 (2001).
21. Caspers, S. *et al.* Organization of the human inferior parietal lobule based on receptor architectonics. *Cereb. Cortex* **23**, 615–628 (2013).
22. Mehta, M. A. *et al.* Methylphenidate enhances working memory by modulating discrete frontal and parietal lobe regions in the human brain. *J. Neurosci.* **20**, RC65 (2000).
23. Gorgoraptis, N. *et al.* The effects of the dopamine agonist rotigotine on hemispatial neglect following stroke. *Brain* **135**, 2478–2491 (2012).
24. Maruff, P., Hay, D., Malone, V. & Currie, J. Asymmetries in the covert orienting of visual spatial attention in schizophrenia. *Neuropsychologia* **33**, 1205–1223 (1995).
25. Silk, T. J., Newman, D. P., Eramudugolla, R., Vance, A. & Bellgrove, M. A. Influence of methylphenidate on spatial attention asymmetry in adolescents with attention deficit hyperactivity disorder (ADHD): preliminary findings. *Neuropsychologia* **56**, 178–183 (2014).
26. Bellgrove, M. A. *et al.* Spatial attentional bias as a marker of genetic risk, symptom severity, and stimulant response in ADHD. *Neuropsychopharmacology* **33**, 2536–2545 (2008).
27. Clark, C. R., Geffen, G. M. & Geffen, L. B. Catecholamines and the covert orientation of attention in humans. *Neuropsychologia* **27**, 131–139 (1989).
28. Bellgrove, M. A. *et al.* Dopaminergic genotype biases spatial attention in healthy children. *Mol. Psych.* **12**, 786–792 (2007).
29. Bellgrove, M. A. *et al.* Dopaminergic haplotype as a predictor of spatial inattention in children with attention-deficit/hyperactivity disorder. *Arch. Gen. Psych.* **66**, 1135 (2009).
30. Newman, D. P. *et al.* Dopamine transporter genotype is associated with a lateralized resistance to distraction during attention selection. *J. Neurosci.* **34**, 15743–15750 (2014).
31. Williams, G. V. & Goldman-Rakic, P. S. Modulation of memory fields by dopamine D1 receptors in prefrontal cortex. *Nature* **376**, 572–575 (1995).
32. Noudoost, B. & Moore, T. The role of neuromodulators in selective attention. *Trends Cogn. Sci.* **15**, 585–591 (2011).
33. Clark, K. L. & Noudoost, B. The role of prefrontal catecholamines in attention and working memory. *Front. Neural Circ.* **8**, 33 (2014).
34. Goris, R. L. T., Movshon, J. A. & Simoncelli, E. P. Partitioning neuronal variability. *Nat. Neurosci.* **17**, 858–865 (2014).
35. Thiele, A., Delicato, L. S., Roberts, M. J. & Gieselmann, M. A. A novel electrode-pipette design for simultaneous recording of extracellular spikes and iontophoretic drug application in awake behaving monkeys. *J. Neurosci. Methods* **158**, 207–211 (2006).
36. Herz, A., Zieglgänsberger, W. & Färber, G. Microelectrophoretic studies concerning the spread of glutamic acid and GABA in brain tissue. *Exp. Brain Res.* **9**, (1969).
37. Jacob, S. N., Ott, T. & Nieder, A. Dopamine regulates two classes of primate prefrontal neurons that represent sensory signals. *J. Neurosci.* **33**, 13724–13734 (2013).

38. Jacob, S. N., Stalter, M. & Nieder, A. Cell-type-specific modulation of targets and distractors by dopamine D1 receptors in primate prefrontal cortex. *Nat. Commun.* https://doi.org/10.1038/ncomms13218 (2016).
39. Vijayraghavan, S., Wang, M., Birnbaum, S. G., Williams, G. V. & Arnsten, A. F. T. Inverted-U dopamine D1 receptor actions on prefrontal neurons engaged in working memory. *Nat. Neurosci.* **10**, 376–384 (2007).
40. Thiele, A. *et al.* Attention induced gain stabilization in broad and narrow-spiking cells in the frontal eye-field of macaque monkeys. *J. Neurosci.* **36**, 7601–7612 (2016).
41. Watanabe, M., Kodama, T. & Hikosaka, K. Increase of extracellular dopamine in primate prefrontal cortex during a working memory task. *J. Neurophysiol.* **78**, 2795–2798 (1997).
42. Ott, T. & Nieder, A. Dopamine and cognitive control in prefrontal cortex. *Trends Cogn. Sci.* **23**, 213–234 (2019).
43. Ott, T., Jacob, S. N. & Nieder, A. Dopamine receptors differentially enhance rule coding in primate prefrontal cortex neurons. *Neuron* **84**, 1317–1328 (2014).
44. Sawaguchi, T. & Goldman-Rakic, P. D1 dopamine receptors in prefrontal cortex: involvement in working memory. *Science* **80**(251), 947–950 (1991).
45. Sawaguchi, T., Matsumura, M. & Kubota, K. Effects of dopamine antagonists on neuronal activity related to a delayed response task in monkey prefrontal cortex. *J. Neurophysiol.* **63**, 1401–1412 (1990).
46. Sawaguchi, T. & Goldman-Rakic, P. S. The role of D1-dopamine receptor in working memory: local injections of dopamine antagonists into the prefrontal cortex of rhesus monkeys performing an oculomotor delayed-response task. *J. Neurophysiol.* **71**, 515–528 (1994).
47. Mueller, A., Shepard, S. B. & Moore, T. Differential expression of dopamine d5 receptors across neuronal subtypes in macaque frontal eye field. *Front. Neural Circ.* https://doi.org/10.3389/fncir.2018.00012 (2018).
48. Mueller, A., Krock, R. M., Shepard, S. & Moore, T. Dopamine receptor expression among local and visual cortex-projecting frontal eye field neurons. *Cereb. Cortex* https://doi.org/10.1093/cercor/bhz078 (2019).
49. Seamans, J. K. & Yang, C. R. The principal features and mechanisms of dopamine modulation in the prefrontal cortex. *Prog. Neurobiol.* **74**, 1–58 (2004).
50. Millan, M., Newman-Tancredi, A., Quentric, Y. & Cussac, D. The 'selective' dopamine D 1 receptor antagonist, SCH23390, is a potent and high efficacy agonist at cloned human serotonin 2C receptors. *Psychopharmacol. (Berl)* **156**, 58–62 (2001).
51. Zahrt, J., Taylor, J. R., Mathew, R. G. & Arnsten, A. F. T. Supranormal stimulation of D 1 dopamine receptors in the rodent prefrontal cortex impairs spatial working memory performance. *J. Neurosci.* **17**, 8528–8535 (1997).
52. Arnsten, A. F. T., Cai, J. X., Murphy, B. L. & Goldman-Rakic, P. S. Dopamine D1 receptor mechanisms in the cognitive performance of young adult and aged monkeys. *Psychopharmacol. (Berl).* https://doi.org/10.1007/BF02245056 (1994).
53. Loewenfeld, I. E. *The pupil: anatomy, physiology, and clinical applications*. (Wayne State University, 1993).
54. McDougal, D. H. & Gamlin, P. D. Autonomic control of the eye. in *Comprehensive physiology* 439–473 (Wiley, Hoboken, 2014). doi:https://doi.org/10.1002/cphy.c140014.
55. Naber, M., Alvarez, G. A. & Nakayama, K. Tracking the allocation of attention using human pupillary oscillations. *Front. Psychol.* https://doi.org/10.3389/fpsyg.2013.00919 (2013).
56. Binda, P. & Murray, S. O. Spatial attention increases the pupillary response to light changes. *J. Vis.* **15**, 1–1 (2015).
57. Binda, P. & Murray, S. O. Keeping a large-pupilled eye on high-level visual processing. *Trends Cogn. Sci.* **19**, 1–3 (2015).
58. Ebitz, R. B. & Moore, T. Selective modulation of the pupil light reflex by microstimulation of prefrontal cortex. *J. Neurosci.* **37**, 5008–5018 (2017).
59. Binda, P. & Gamlin, P. D. Renewed attention on the pupil light reflex. *Trends Neurosci.* **40**, 455–457 (2017).
60. Wang, C.-A., Boehnke, S. E., White, B. J. & Munoz, D. P. Microstimulation of the monkey superior colliculus induces pupil dilation without evoking saccades. *J. Neurosci.* **32**, 3629–3636 (2012).
61. Joshi, S., Li, Y., Kalwani, R. M. & Gold, J. I. Relationships between pupil diameter and neuronal activity in the locus coeruleus, colliculi, and cingulate cortex. *Neuron* **89**, 221–234 (2016).
62. Kustov, A. A. & Lee Robinson, D. Shared neural control of attentional shifts and eye movements. *Nature* **384**, 74–77 (1996).
63. Ignashchenkova, A., Dicke, P. W., Haarmeier, T. & Thier, P. Neuron-specific contribution of the superior colliculus to overt and covert shifts of attention. *Nat. Neurosci.* **7**, 56–64 (2004).
64. Muller, J. R., Philiastides, M. G. & Newsome, W. T. Microstimulation of the superior colliculus focuses attention without moving the eyes. *Proc. Natl. Acad. Sci.* **102**, 524–529 (2005).
65. Lovejoy, L. P. & Krauzlis, R. J. Inactivation of primate superior colliculus impairs covert selection of signals for perceptual judgments. *Nat. Neurosci.* **13**, 261–266 (2010).
66. McPeek, R. M. & Keller, E. L. Deficits in saccade target selection after inactivation of superior colliculus. *Nat. Neurosci.* **7**, 757–763 (2004).
67. McPeek, R. M. & Keller, E. L. Saccade target selection in the superior colliculus during a visual search task. *J. Neurophysiol.* **88**, 2019–2034 (2002).
68. Mysore, S. P. & Knudsen, E. I. The role of a midbrain network in competitive stimulus selection. *Curr. Opin. Neurobiol.* **21**, 653–660 (2011).
69. Kuypers, H. G. J. M. & Lawrence, D. G. Cortical projections to the red nucleus and the brain stem in the rhesus monkey. *Brain Res.* **4**, 151–188 (1967).
70. Becker, W. The neurobiology of saccadic eye movements. *Metrics. Rev. Oculomot. Res.* **3**, 13–67 (1989).
71. Wang, C.-A. & Munoz, D. P. A circuit for pupil orienting responses: implications for cognitive modulation of pupil size. *Curr. Opin. Neurobiol.* **33**, 134–140 (2015).
72. Robbins, T. W. & Arnsten, A. F. T. The neuropsychopharmacology of fronto-executive function: monoaminergic modulation. *Annu. Rev. Neurosci.* **32**, 267–287 (2009).
73. Gray, H. *et al.* Physiological, behavioral, and scientific impact of different fluid control protocols in the rhesus macaque (*Macaca mulatta*). *Eneuro* **3**, 1–15 (2016).
74. Gieselmann, M. A. & Thiele, A. Comparison of spatial integration and surround suppression characteristics in spiking activity and the local field potential in macaque V1. *Eur. J. Neurosci.* **28**, 447–459 (2008).
75. van Kempen, J. *et al.* Top-down coordination of local cortical state during selective attention. *Neuron* https://doi.org/10.1016/j.neuron.2020.12.013 (2021).
76. Ferro, D., van Kempen, J., Boyd, M., Panzeri, S. & Thiele, A. Directed information exchange between cortical layers in macaque V1 and V4 and its modulation by selective attention. *Proc. Natl. Acad. Sci.* **118**, e2022097118 (2021).
77. Distler, C. & Hoffmann, K.-P. Cortical input to the nucleus of the optic tract and dorsal terminal nucleus (NOT-DTN) in macaques: a retrograde tracing study. *Cereb. Cortex* **11**, 572–580 (2001).
78. Ardid, S. *et al.* Mapping of functionally characterized cell classes onto canonical circuit operations in primate prefrontal cortex. *J. Neurosci.* https://doi.org/10.1523/JNEUROSCI.2700-14.2015 (2015).
79. Green, D. M. & Swets, J. A. *Signal detection theory and psychophysics*. (Wiley, Hoboken, 1966). doi:https://doi.org/10.1901/jeab.1969.12-475.
80. Bates, D., Mächler, M., Bolker, B. & Walker, S. Fitting linear mixed-effects models using lme4. *J. Stat. Softw.* **67**, (2015).
81. Kuznetsova, A., Brockhoff, P. B. & Christensen, R. H. B. lmerTest package: tests in linear mixed effects models. *J. Stat. Softw.* **82**, (2017).

82. Halekoh, U. & Højsgaard, S. A Kenward-Roger approximation and parametric bootstrap methods for tests in linear mixed models: the R package pbkrtest. *J. Stat. Softw.* **59**, 1–32 (2014).
83. Kenward, M. G. & Roger, J. H. Small sample inference for fixed effects from restricted maximum likelihood. *Biometrics* **53**, 983 (1997).
84. Singmann, H. & Kellen, D. An introduction to mixed models for experimental psychology. in *New Methods in Cognitive Psychology* 4–31 (Routledge, New York, 2019). doi:https://doi.org/10.4324/9780429318405-2.
85. Andraszewicz, S. *et al.* An introduction to bayesian hypothesis testing for management research. *J. Manag.* **41**, 521–543 (2015).
86. Rouder, J. N. & Morey, R. D. Default bayes factors for model selection in regression. *Multivar. Behav. Res.* **47**, 877–903 (2012).
87. Morey, R. D. & Rouder, J. N. BayesFactor: computation of bayes factors for common designs. (2018).
88. Simonsohn, U. Two-lines: a valid alternative to the invalid testing of U-shaped relationships with quadratic regressions. *Ssrn* https://doi.org/10.2139/ssrn.3021690 (2017).
89. Bechtold, B. Violin plots for Matlab. Github Project. https://doi.org/10.5281/zenodo.4559847 (2016).
90. van Kempen, J., Brandt, C. & Thiele, A. Macaque Posterior Parietal Cortex recordings during iontophoretic dopaminergic drug application, *G-Node*, https://doi.org/10.12751/g-node.7ni115 (2022).

Acknowledgements

This work was supported by Wellcome trust [093104] (JvK, AT), MRC [MR/P013031/1] (JvK, AT); by a Senior Research Fellowship from the Australian National Health and Medical Research Council (NHMRC) (MAB); and by a strategic research partnership between Newcastle University and Monash University (JvK, MAB, AT).

Author contributions

Conceptualization, J.K., M.B., A.T.; Methodology, J.K., A.T.; Formal analysis, J.K., A.T.; Investigation, J.K., C.B., C.D., A.T.; Data Curation, J.K., A.T., Software, J.K.; Writing—original draft preparation, J.K., Writing—review and editing, J.K., C.B., C.D., M.B., A.T.; Resources, M.B., A.T.; Supervision, M.B., A.T.; Funding acquisition, M.B., A.T.; Visualization, J.K.

Competing interests

The authors declare no competing interests.

Additional information

Supplementary Information The online version contains supplementary material available at https://doi.org/10.1038/s41598-022-10634-w.

Correspondence and requests for materials should be addressed to J.K.

Reprints and permissions information is available at www.nature.com/reprints.

Publisher's note Springer Nature remains neutral with regard to jurisdictional claims in published maps and institutional affiliations.